Energy 239 (2022) 122349

Contents lists available at ScienceDirect

Energy

journal homepage: www.elsevier.com/locate/energy

The contribution of L-Arginine to the mass transfer performance of CO_2 absorption by an aqueous solution of methyl diethanolamine in a microreactor

Shokouh Sarlak, Peyvand Valeh-e-Sheyda*

Chemical Engineering Department, Kermanshah University of Technology, Kermanshah, Iran

ARTICLE INFO

Article history:
Received 27 June 2021
Received in revised form
22 September 2021
Accepted 15 October 2021
Available online 21 October 2021

Keywords:
Absorption
Arginine
CO_2 mass transfer flux per unit volume
Overall gas-phase mass transfer coefficient
Methyldiethanolamine
Microchannel

ABSTRACT

The current study investigates the effect of adding L-arginine as a potential promoter for the conventional methyl diethanolamine (MDEA) in the carbon dioxide (CO_2) capture process in a T-junction microreactor. The overall gas-phase mass transfer coefficient ($K_G a_V$) and CO_2 absorption efficiency (e_f) were evaluated under distinct operating conditions, including total amine + amino acid concentration of 50 wt%, the liquid flow rate of 3–9 mL min^{-1}, and gas flow rate of 120–300 mL min^{-1}. The composition of different concentrations in the mixture were as MDEA (50%), MDEA + ARG (46 + 4%), MDEA + ARG (42 + 8%),MDEA + ARG (38 + 12%). The impact of amino acid concentration on the physical properties of the aqueous MDEA solution was also compared in four solutions. The results indicated that increasing the arginine concentration from 4 wt% to 12 wt% intensifies the e_f values from 78.91 to 92.7%, while the solution density and viscosity grows slightly. Furthermore, the values of the $K_G a_V$ in the CO_2 absorption enhanced from 14.34 kmol/(m^3 kPa h) in aqueous MDEA (50%) solution to 63 kmol/(m^3 kPa h) in MDEA + ARG (38 + 12%). It confirmed that arginine could apply as a potential chemical activator in the mixture of MDEA-ARG to intensify the absorption of CO_2 in the post-combustion CO_2 capture processes.

1. Introduction

In the recent decade, considerable quantities of acid gases such as CO_2 in the crude natural gas has been recognized as one of the major issues regarding the fuel quality and social and environmental concern [1]. The excessive emission of CO_2, as the main greenhouse gas, has caused serious global greenhouse effect. The Carbon Capture and Sequestration (CCS) is an effective technology, enabling the reduction of CO_2 emission into atmosphere. Typically, there are two strategies to intensify the economic efficiency of CO_2 capture; first, the utilization of the modern, efficient reactors and second, the development of novel solvents with improved reaction kinetics [2]. In this regards, the commercial application and economic efficiency of many types of gas-liquid mass transfer contactors are confined by their vast volume, low efficiencies, high regeneration energy requirement, and operating cost. The microchannel technology, as a novel effective micro-mixing technology with a fast mass transfer process and short residence time, can provide distinguished merits such as increasing safety, intensifying process, process control improvement, as compared with traditional gas-liquid contactors [3]. Besides, the high specific surface area yields intensification of mass and heat transfer and boost the absorption efficiency [4]. These merits make the implementation of these simple contacting structures much safer in practice.

Regarding the second strategy, aqueous solutions of alkanolamines are the most broadly employed solvents in post-combustion CO_2 capture in many petrochemical industries [5,6]. Among the amine-based solvents used in these gas treatment processes, methyl diethanolamine (MDEA), as a tertiary alkanolamine possesses such characteristics as low vapor pressure, resistant to thermal and chemical degradation, high loading capacity (1 mol CO_2 per mole amine), high H_2S selectivity, low regeneration energy, and less corrosion [7]. Besides, tertiary alkanolamines (MDEA) do not produce stable carbamate, requiring more heat to break; alternatively, they make bicarbonate that needs lower heat compared to carbamate, leading to lower costs of the absorbent regeneration. On the other side, the rate of bicarbonate formation ions is comparatively slow compared to the formation of carbamate ion, so the CO_2 capture kinetics in tertiary amines is usually slower

* Corresponding author.
E-mail address: p.valeh-sheyda@kut.ac.ir (P. Valeh-e-Sheyda).

https://doi.org/10.1016/j.energy.2021.122349
0360-5442/

than that for primary and secondary amines [8]. Ultimately, the reaction heat of MDEA is relatively low with CO_2, which makes it potential to reduce the reboiler heat duty, thus reducing operating costs. However, low viscosity, foaming formation, and slow rate of carbon dioxide absorption have been presented as some significant drawbacks of the tertiary alkanolamine in separation systems.

To tackle these problems, it is suggested to add a co-promoter to the conventional alkanolamines systems. Unique properties of amino acids such as the less toxic opposite of amines and known to resist oxidative degradation have made them a noteworthy alternative for solvent-based absorption systems [9–12]. Amino acids, known as 2-, alpha-, or α-amino acids, have both the amine (NH_2) and the carboxylic acid (−COOH) groups connected to the alpha-(first) carbon atom [13,14]. The presence of an extremely basic guanidine side chain in arginine makes it as the most basic amino acid, expected to exhibit superior CO_2 absorption capacity, as compared with other amino acids. Due to the strong basic chain in the basic environment, it is expected to have high reactivity and capacity compared with the primary amines [15].

Over the recent years, numerous studies in the literature have investigated the gas-liquid absorption process utilizing alkanolamine solutions in the microreactors. Ganapathy et al. [16] studied the fluid flow and mass transfer characteristics of absorbed CO_2 into DEA solution in a micro-structured absorber. The mass transfer of chemical absorption was investigated from the N_2/CO_2 mixture in the binary mixtures of 5, 10, 15 and 20 wt% MDEA with 4 wt% activator piperazine (PZ). The liquid-side volumetric mass transfer coefficient (k_La) and CO_2 absorption percentage reached 1.70 s^{-1} and 97%, respectively, at gas flow rate of 100 L/h and liquid flow rate of 5.32 L/h using blending (10 + 4 wt%) MDEA-PZ [3]. The usage of a non-aqueous solution of 2-amino-2-methyl-1-propanol (AMP) + ethylene glycol (EG) was investigated in a microreactor. The results indicated that the mass transfer coefficient in the contacting microstructured device was higher than that in the conventional absorber column, and AMP concentration had a direct relation with mass transfer coefficient [17]. Lin et al. [18] investigated the mass transfer efficiency of the aqueous blend of MDEA (5 wt%) with DEA (1–5 wt%) and CO_2 in a T-junction microreactor. They found that the increasing DEA concentration accelerated the chemical reaction rate of absorbed CO_2 into liquid, leading to the enhancement of CO_2 removal efficiency and mass transfer coefficient. Ma et al. [19] applied MEA blended with N, N-diethylethanolamine (DEEA) to investigate gas-liquid phase flow and the mass transfer performance of CO_2 capture into a microreactor. They achieved the liquid-side overall volumetric mass transfer coefficient (k_La) in the range of 3.04–20.07 s^{-1}, which was 2–3 times higher than traditional devices.

Considering the promising application of L-arginine and other basic amino acids for post-combustion carbon capture, knowledge of the physicochemical properties of the amino acid solutions is crucial to design the absorption columns in the CO_2 capture processes, as they are connected to the mass transfer coefficients. As an illustration, numerous computations such as mass transfer, fluid flow, etc., need the knowledge on the viscosity at the beginning of this section [20]. The density of a solvent is a crucial physical property for the examination of reaction kinetics and mass transfer, as well as the prediction of the CO_2 solubility in the solvent. However, the available information on the effectiveness of the arginine amino acid as a co-solvent with a three-carbon aliphatic straight-chain is not well defined on the augmentation of the mass transfer characteristics of a tertiary alkanolamine, MDEA, in microchannels. Besides, the physico-chemical properties of the aqueous MDEA + L-arginine have not been reported, yet and require to be informed.

Concerning the performance of the amino acids for CO_2 capture, in the present study, a basic amino acid, L-arginine, is introduced as a promising absorbent for aqueous MDEA solution in the microchannel. Using amino acid-based solutions, some of the physicochemical properties required, including density, and viscosity are experimentally measured. Besides, the mass transfer performance of the suggested novle solvent, MDEA + ARG, is investigated in the microreactor. The impact of gas and blended solvent flow rates, as well as the contribution of L-arginine on the CO_2 absorption efficiency and volumetric mass transfer coefficient, are examined at the constant operating temperature of 45 °C under atmospheric pressure. Finally, the obtained values of the K_{GaV} for the blend of the amino acid and MDEA in the microchannel reactor is compared with the performance of the alkanolamine base solvent in the absorption packed columns.

2. Theory

2.1. Reaction mechanism of CO_2 with promoted MDEA solution

The chemical equilibrium reactions of CO_2 with ARG and MDEA (RR′R″N, where R‴ = CH_3 and R′ = R″ = C_2H_4OH), as a tertiary amine, for MDEA-ARG−H_2O−CO_2 systems are given as follows [21]:

$$CO_2 + H_2O \leftrightarrow HCO_3^- + H^+ \quad (1)$$

$$HCO_3^- \leftrightarrow CO_3^{2-} + H^+ \quad (2)$$

$$H_2O \leftrightarrow OH^- + H^+ \quad (3)$$

$$RR'R''NH^+ \leftrightarrow RR'R''N + H^+ \quad (4)$$

As seen in Eqs. (1) and (2), carbonate and bicarbonate ions are formed in aqueous systems by dissociating CO_2 into water. In the next step, the water is ionized, and the protonated MDEA amine dissociates through Eqs. (3) and (4). It is noted that during the reactions of CO_2 with tertiary amines, the stable carbamate is not formed, as needs more heat for the breakage; alternatively, they produce bicarbonate, which needs lower heat than carbamate, leading to a decrease in the costs of the solvent regeneration [22].

The molecular structure of amino acid; hence, the reaction pathway of CO_2-amino acid is also similar to that of CO_2-amine according to the zwitterion mechanisms [23]. If the amino acid ARG ($^+NH_3RCOO^-$), in which R is an organic substituent called as a 'side chain), is dissolved in water, the amino group will be completely deprotonated (Eq. (5)), and the carbamate is formed (Eq. (6)).

$$^+N\,H_3RCOO^- + H_2O \leftrightarrow H_3O^+ + NH_2RCOO^- \quad (5)$$

$$HCO_3^- + {}^-OOCRNH_2^+ \leftrightarrow -OOCRNHCOO^- + H_2O \quad (6)$$

2.2. Error analysis

The precision of the experimental measurements has been determined from the repeatability of the measured quantities. For a set of N measured quantities of physical property, e.g., x_i, the uncertainty values are defined from:

$$\mu = \frac{1}{N}\sum_{i=1}^{N} x_i \quad (7)$$

$$\sigma_x = \sqrt{\frac{1}{N-1}\sum_{i=1}^{N}(x_i-\mu)^2} \tag{8}$$

According to the above correlations, μ and σ_x describe the mean of the experimental measurements and the population standard deviation, respectively. The relative magnitude of the standard deviation (*RSD*) is also calculated as follows:

$$RSD\ (\%) = 100\frac{\sigma_x}{\mu} \tag{9}$$

The measured quantities can be noted as $x = \mu \pm RSD\ (\%)$ or $x = \mu \pm \sigma_x$.

2.3. Indicators of the mass transfer efficiency (K_Ga_V, e_f, N_Aa_V)

The overall gas-phase mass transfer coefficient (K_Ga_V) and the CO_2 absorption efficiency (e_f) are typically recognized as the practical responses to analyze the CO_2 absorption performance. The mass flux per unit volume of the CO_2 absorption (N_Aa_V) into the solvent can be defined in terms of the total pressure of the system (P) and driving force ($y_{A,G} - y_A^*$), as follows [24]:

$$N_Aa_V = K_Ga_VP\left(y_{A,G} - y_A^*\right) \tag{10}$$

where $y_{A,G}$ and y_A^* denote the mole fractions of CO_2 in the gas-phase and equilibrium concentration of CO_2 at the interface. P and a_V express the total pressure and interfacial area per volume (m^2/m^3), respectively.

Regarding the absorption process happens in any length element, dh, the overall differential mass balance is demonstrated as follows:

$$N_aa_V dh = G_1 dY_A \tag{11}$$

where Y_A and G_1 express the mole ratio of component A and molar flow rate of inert gas, respectively. Incorporating Eqs. (10) and (11), one can obtain a simplified correlation to calculate the total mass transfer coefficient in the gas phase in terms of K_Ga_V (kmol/m^3.h.kPa):

$$K_Ga_V = \frac{G}{HP}\left[ln\left(\frac{Y_{A,in}}{Y_{A,out}}\right) + \left(Y_{A,in} - Y_{A,out}\right)\right] \tag{12}$$

where, $Y_{A,in}$ and $Y_{A,out}$ represent the mole ratio of CO_2 at the inlet and outlet of the microreactor. Besides, P, G and H are the system pressure (kPa), the inlet gas flow rate (kmol/h.m^2) and the length of the microreactor (m), respectively.

For the present work, the CO_2 absorption efficiency can be calculated as below:

$$e_f = \frac{y_{in} - y_{out}}{y_{in}} \times 100 \tag{13}$$

where e_f is the CO_2 absorption efficiency, y_{in} and y_{out} represent the CO_2 mole fractions in the gas stream at the entry and exit of the microreactor.

For more considerations, the volumetric mass transfer flux per unit volume (N_Aa_V) was calculated based on the two-film theory, as presented in Fig. 1. In the two-film theory, it is presumed that the liquid and vapor phases both are composed of thin film and bulk regions, and all of the resistance to the mass transfer is accumulated in the thin boundary layer next to the phase interphase [25]. As such, under the steady-state condition, the mass transfer occurs

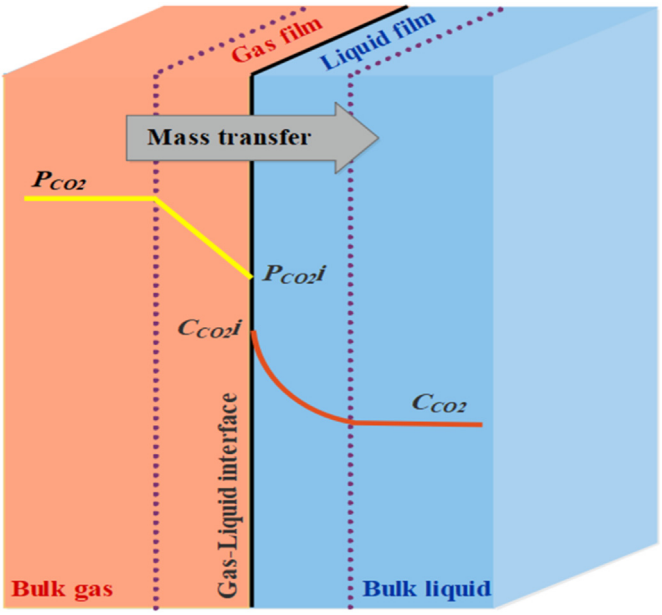

Fig. 1. The schematic diagram of the two-film mass transfer theory of CO_2 absorption [28].

as the CO_2 moves from the gas phase across a static film into the liquid phase owing to the driving force ($y_{A,G} - y_A^*$). For a fast chemical reaction, the value of y_A^* is very close to zero and usually neglected in the amine scrubbing to remove CO_2 [26]. Finally, considering the overall material balance at the entrance and exit of the microreactor, whose concentrations are $Y_{CO_2,in}$ and $Y_{CO_2,out}$, the mass flux per unit volume of the CO_2 absorption, N_Aa_V, can be written as:

$$N_Aa_V = \frac{G}{Z}\left(Y_{CO_2,in} - Y_{CO_2,out}\right) \tag{14}$$

where G represents the inert gas flow rate, kmol/h.m^2; Y_{CO_2} exhibits the mole ratio of CO_2 in the bulk gas, kmol CO_2/kmol air, respectively [27].

The mass transfer rate enhanced by the aqueous blended solution of MDEA and amino acid was expressed applying the prompter efficiency, which is the ratio of the volumetric mass transfer flux per unit volume for the aqueous blended solution of MDEA + ARG, $N_{(M+A)}a_V$, to the corresponding value obtained for the aqueous solutions of MDEA N_Ma_V. The promoter efficiency is represented by the following equation:

$$Promoter\ efficiency = \frac{N_{(M+A)}a_V}{N_Ma_V} \tag{15}$$

3. Material and methods

3.1. Material

In this study, CO_2 with 99.9% purity was provided from Alborz Persian Gas, Karaj, Iran. The obtainable industrial methyl diethanolamine (MDEA) and L-arginine (ARG) with 99.0% purity were supplied from Ilam Gas Company and Merck KGaA, respectively. The molecular structure of the tertiary amine, MDEA, and the organic amino acid, L-arginine, are illustrated in Fig. 2.

To prepare the aqueous solutions, the appropriate concentration

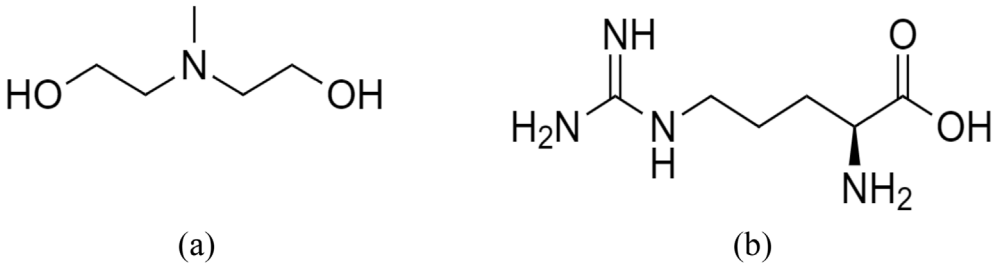

Fig. 2. The 2D molecular structures of (a) methyl diethanolamine ($CH_3N(C_2H_4OH)_2$) and (b) L-arginine ($C_6H_{14}N_4O_2$).

of MDEA and L-arginine was dissolved in the deionized water at room temperature.

3.2. Experimental apparatus

The schematic sketch of the CO_2 absorption experimental setup applied in the present work is illustrated in Fig. 3. A T-shape microreactor, made of transparent plastic, was assumed with a diameter of 800 μm and a length of 295 mm. The microreactor is positioned in the water bath, equipped with a recirculation pump, to govern the bath temperature at the given set point. A digital thermometer (Lutron BTM-1644208SD, K type, ±0.1 K) was applied to control the temperature of the feeding fluid by immersing the coiled feeding tubes in the water circulating bath.

Two Mass Flow controllers (GPC series, Iran) monitored the inlet flow rates of the gas phase, including air and CO_2, before mixing. The inlet CO_2 flow was supplied from a gas cylinder, while the air was provided from an air compressor, BA-1006 M, China. A peristaltic pump (BT-100-1 F, China) applied to control and inject the solvent into the microchannel test section. Eventually, the gas-liquid mixture, leaving the microreactor, entered a collector. Two digital CO_2 analyzers (COZIR-WR sensor, Germany) were applied to measure the CO_2 content in the gas feed and product. The CO2 meter (CM-0123 20%) can measure CO2 concentrations from 0 to 20% with an error of less than 0.01%. The measured CO_2 data were recorded every 5 s via a PC. Table 1 outlines the utilized substantial components as well as the technical details of the experimental setup.

3.3. Experimental procedure

Initially, the air and CO_2 streams are individually adjusted by the MFCs to obtain the total specified flow rates at 15% v/v of CO_2. Once the desired percentage of CO_2 in the inlet feed gas reached, the content of CO_2 in the inlet flue gas is recorded using a digital CO_2 analyzer. To wet the feed gas with the vapours of the aqueous MDEA + ARG solution, the gas stream is passed through a bubbling flask containing water. Then, two coiled tubes are placed into the water bath and connected to both gas and liquid inlets to attain the given temperature. The prepared aqueous solutions of the desired concentrations are then continuously fed to the test section via a peristaltic pump. The gas and liquid streams feed simultaneously to the T-shaped microreactor, where the CO_2 capture process would occur. To reach the steady-state condition, the subsequent decline in the CO_2 concentration in the outlet stream along the micro-channel is measured versus time and recorded in a PC via a data

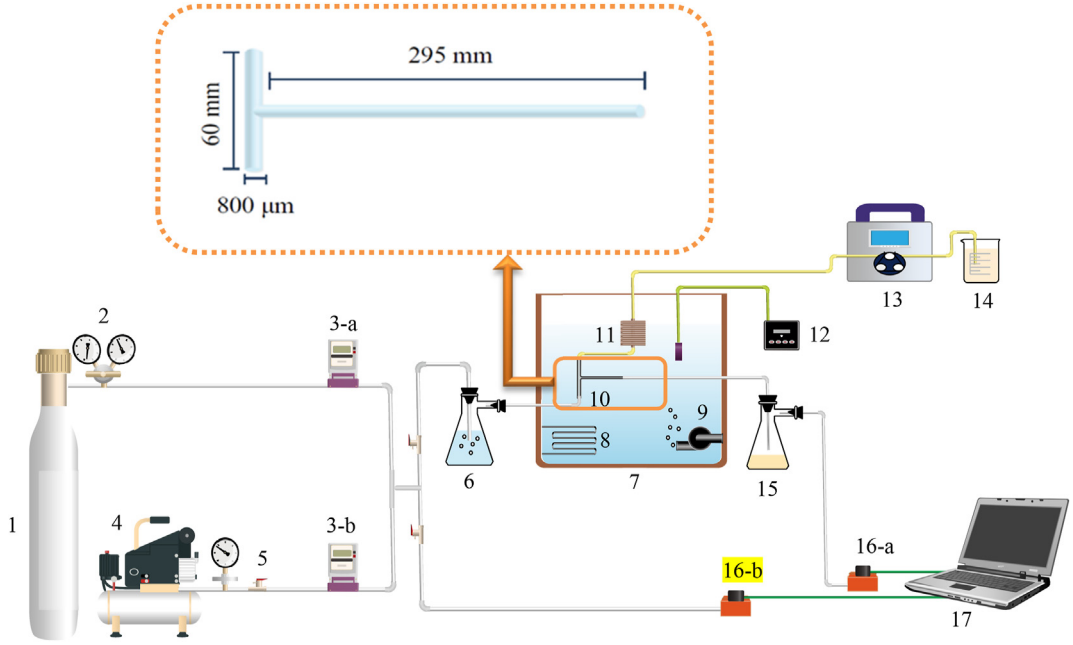

Fig. 3. Schematic sketch of the CO_2 absorption experimental setup: (1) CO_2 cylinder, (2) Pressure gage, (3) Mass Flow Controller (MFC), (4) Air compressor, (5) Valve, (6) Gas humidification chamber, (7) Water bath, (8) Heater, (9) Pump, (10) Microreactor, (11) Coil, (12) Thermometer, (13) Peristaltic pump, (14) Fresh solvent injection tank, (15) Solvent outlet, (16) CO_2 sensor, (17) PC system.

Table 1
The main constituents and properties of the experimental setup.

Component	Model No.	Company
Microreactor	Length = 295 mm Diameter = 800 μm	–
Air compressor	BA-1006 M	OMEGA tools, China
Peristaltic pump	BT-100-1 F	China
Mass Flow Controller (MFC)-Air	GPC series-BREEZENS	Apasco, Iran
Mass Flow Controller (MFC)-CO_2	GPC series-BREEZENS	Apasco, Iran
CO_2 sensor	CM-0123	COZIR-WR, Germany
Thermometer	BTM-4208 SD, LUTRON	–

logger. All experiments were carried out under atmospheric pressure and 15% CO_2 in the inlet gas stream. To assure the accuracy of the experiment, the experiments were repeated.

3.4. Gas-liquid flow pattern

The distribution of the flow pattern was demonstrated considering the operating range of experimental tests, defined for CO_2 absorption into MDEA-ARG aqueous solution. As presented in Fig. 4, the gas-liquid flow patterns were plotted based on the previous studies reported by Chung and Kawaji [29]. Based on the earlier studies [30,31], it was notices that changing the flow rates of gas and liquid phases generates different dominating force, which influences the mechanism of the bubble formation inside the microreactor. Accordingly, for microreactors with diverse geometries, the flow regimes can be divided into three regions, including churn flow, slug flow and slug-annular flow.

Based on the figure, it is evident that the slug flow mainly appears as the gas velocity is low while the liquid velocity is relatively high. The results of the gas-liquid mass transfer characteristics in flow regime maps confirmed that the annular flow gives the highest mass transfer coefficient [32]. Applying the visualization method, the bubble shape and length have been characterized in the work of Ma et al. [33]. However, at higher gas-phase flow rates, where the gas phase superficial velocity is larger than 10 m/s, the flow pattern would develop into the slug-annular flow. This speculation confirmed that at a given liquid flow rate, where the fluid superficial velocity is less than 1 m/s, raising the gas-phase flow improves the bubble velocity and the effective mass transfer area [34,35]. Under the experimental gas-liquid operating conditions, this study has been primarily concentrated on the mass transfer process of CO_2 absorption in the aqueous solution of MDEA + ARG under the slug-annular flow.

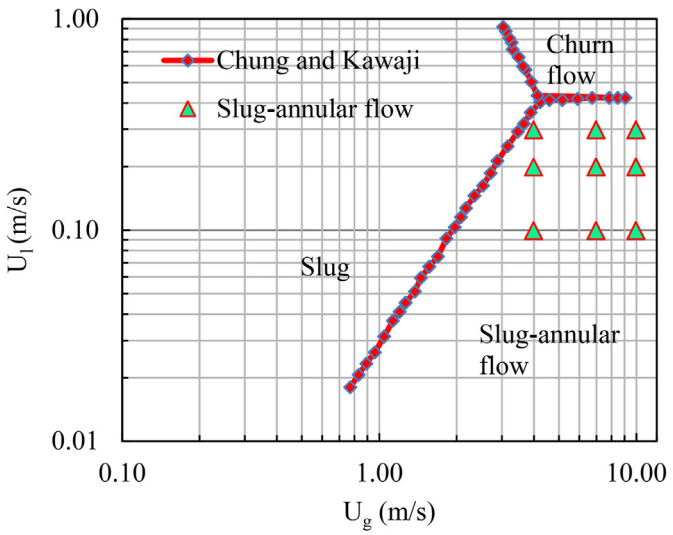

Fig. 4. The flow pattern map for the microreactor with 800 μm diameter.

3.5. Operating conditions

Concerning industrial limitation and requirements, the four operating variables with the significant impact on the absorption process were considered in the microreactor. Table 2 summarizes the operating variables and their corresponding ranges considered in the present study. Considering the parameters limiting further increase in MDEA concentration in the solvent for CO_2 post-combustion in the gas refinery industry, the total amine concentration (MDEA + amino acid) was kept at the fixed 50 wt%. In this regard, the following compositions of the MDEA were replaced by ARG, as a chemical activator, to examine the contribution of L-arginine to the mass transfer performance of carbon dioxide absorption: MDEA (50 wt%), MDEA + ARG (46 + 4 wt%), MDEA + ARG (42 + 8 wt%), and MDEA + ARG (38 + 12 wt%).

Besides, Considering maximum absorption in the slug-annular flow pattern, the mass flow rate of gas-phase (Qg) and liquid-phase flow rate (Ql) were set in the range of 120–300 mL/min and 3–9 mL/min, respectively [36]. All tests were managed at atmospheric pressure and under an isothermal absorption temperature of 45 °C.

3.6. Physicochemical properties

Typically, to provide operational directions, the optimization of acid gas treatment equipment and the design of capture processes, the physical properties of the absorbents are required. The physicochemical properties of the four concentrations of the MDEA + ARG, namely density, and viscosity have been determined under atmospheric pressure at a fixed temperature of 45 °C to meet the property requirements of the proposed amine + amino acid solution.

To measure the density property of the aqueous blended solvents (amine + amino acid), a pycnometer with a minimal amount of sample was employed. The pycnometer is weighed while empty, filled with the desired sample and allowed to equilibrate thermally at 45 °C. The pycnometer is weighed and the density is then

Table 2
Experimental operating conditions for the absorption process.

Parameter	Value
Absorption solvent	Aqueous MDEA + ARG solution
Feed CO_2 (vol%)	15
Gas flow rate (mL/min)	120–300
Liquid flow rate (mL/min)	3–9
MDEA concentration (wt%)	38–50
Arginine concentration (wt%)	4–12
Temperature (°C)	45

calculated by dividing the mass of the solution of interest by the pycnometer volume. The density of the aqueous MDEA solution was further compared with the results published in the literature to confirm the validation of experiments. The kinematic viscosity is directly determined via a capillary viscometer (model C-100, No. 596, Cannon-Fenske, Japan) immersed in a constant-temperature circulating bath to precisely regulate the solution temperature with the accuracy of ±0.1 K. Reproducibility was certified by running three replicates for each measurement, and all the data presented in the figures are the average of the three trials. The uncertainty values of the experimental physical properties have been reported for different concentrations of the blend of amino acid and MDEA in Table 3.

4. Results and data analysis

4.1. Physical properties of the aqueous solutions

4.1.1. Density and viscosity measurements

The measurements of density and viscosity were carried out at 45 °C for the various MDEA and amino acid mixtures, as are listed in Fig. 5. From the table, it is seen that the experimental values determined for density and viscosity of MDEA 50 wt% are in strong agreement with that in the work of Karunarathne et al. and Arachchige et al. confirming the accuracy of the test rig [37]. As seen, the densities of the solutions rise as the amino-acid concentration increases from 4 to 12 wt%. It is of note that the density values of MDEA is close to that of water, and the mixture density is primarily affected by the arginine density (1.3 gr/cm^3), which is higher compared with the aqueous MDEA solution. This is supposed mainly due to the enhancement of the hydrogen bond strengths between the molecules [38].

The viscosity measurements have also been investigated for aqueous MDEA 50 %wt solution promoted with ARG 0−12 wt% with different ratios. As seen, the values for all the mixtures studied were in the range of 4.29−5.15 mm^2/s. The present measured viscosities of the MDEA 50 wt% solution were also compared with published literature [39]. It seems that the presence of impurities and water content in the tertiary amine may lead to the slight discrepancies in the values. It is observed that the viscosity tends to rise with adding the weight percent of ʟ-arginine. It is seen that under atmospheric pressure, the highest viscosity belongs to the MDEA + ARG (38% + 12%) with the maximum value of 5.15 mm^2/s, followed by 42% + 8% (4.97 mm^2/s). The reason may be attributed to the formation of large number of hydrogen bonds between MDEA and ʟ-arginine molecules since the viscosity is mainly affected by the hydrogen bonding.

4.2. Effect of MDEA and ARG concentrations

Referring to the amount of free active absorbent molecules, the amine concentration performs a vital part in the mass transfer characteristics of the aqueous blended MDEA-ARG-based CO_2 absorption. To assess the effect of ʟ-arginine in the total blend solution the efficiency of CO_2 absorption (e_f) and the overall gas-phase mass transfer coefficient ($K_G a_V$) were measured for different binary solutions of MDEA ARG (46 4 wt%), MDEA ARG (42 8 wt%), and MDEA ARG (38 12 wt%), at a total concentration of 50 wt%. Fig. 6a and b demonstrates the results, compared with that of MDEA 50 wt % for the gas-phase flow rate of 210 mL/min.

The figure illustrates that at a given level of liquid flow rate (Q_l = 6 mL/min), by increasing the amino acid weight percent, the value of the $K_G a_V$, as well as the CO_2 absorption efficiency, will be intensified. As an illustration, at a constant gas flow rate of Qg = 210 mL/min, and liquid flow rate of Q_l = 6 mL/min, by raising the arginine concentration from 4 wt% to a level of 12 wt%, the value of e_f has been improved from 78.91% to 92.70%. Under the same experimental operating concentrations, the values of $K_G a_V$ for three levels of MDEA concentrations are approximately calculated 34.4, 43.8, and 55.1 kmol/m^3 h kPa, respectively.

Two possible reasons were considered for arginine as the promoter in the enhancement of CO_2 absorption in the aqueous MDEA solutions. One is that arginine contains a primarily amino functional groups which let it have a fast rate of reaction with CO_2. As such, based on Eqs. (5) and (6), the zwitterion reaction mechanism is generally and the carbamate formation is a significant step [5]. The other is that the basic character of arginine is considered; fast deprotonation from the CO_2-amino acid complex by basic guanidinium group is expected and resulted in carbamate formation and the enhancement of the CO_2 chemical reaction rate [41].

In spite of the fact that increasing the amino acid concentration from 4 to 12 wt%in the mixture can lead to the enlargement of the liquid viscosity 1.2 times higher than the aqueous MDEA solution, as indicated in Fig. 5, this will boost the shear stress on the neck of the bubbles and facilitates the creation of stable bubbles [42]. That is why the values of the e_f and $K_G a_V$ are stepped up as the amino acid concentration increased. The findings are in line with the observations of the earlier works, representing that ARG can essentially enhance the solubility when blends with MDEA [21].

4.3. Effect of solvent flow rate (Q_l)

Fig. 7 gives the obtained values for the CO_2 absorption efficiency (e_f) and overall mass transfer coefficient ($K_G a_V$) when the liquid flow rates varies in the range of 3−9 mL/min. It is noticed that increasing the solvent flow rate from 3 to 9 mL/min enhances the values of the e_f and $K_G a_V$. This significant improvement may be ascribed to the fact that rising the solvent flow rate keeps the concentration of MDEA and/or ʟ-arginine inside the microchannel higher. This will not only grant more active amine molecules in the mixture but will also intensify the interfacial area between the solvent and gas phases, thereby leading to the augmentation of the two key responses [43].

On the other hand, the possible explanation for this behaviour may be assigned to the prevalent flow patterns; in slug-annular flow, higher values of the solvent flow rate will shift the boundaries of the flow regimes towards the up and increase the convective mixing within the liquid slugs. This will reduce the void fractions of the gas, leading to the thicker liquid films in the slug-annular flow. Correspondingly, the slow saturation of the alkanolamine + amino acid reactant adjacent to the gas core discloses the observed trend of rising the $K_G a_V$ in the case of liquid-phase controlled mass transfer [16,44].

However, at high concentrations of the alkanilamine + amino acid solution (38 12 wt%), the slope of the CO_2 absorption efficiency line is relatively high, as the solvent flow rate was less than 6 mL/min and increased slightly as the CO_2 absorption efficiency reaches the maximum level of 94.37% inside the microchannel. In this regard, the enhancement in CO_2 absorption efficiency with the liquid flow rate becomes more meaningful at the low total concentrations of the MDEA-ARG binary mixture. The major contributing factor is

Table 3
The uncertainty values over the experimental measurements.

Parameter	RDS (%)
Density	0.033
Viscosity	0.33

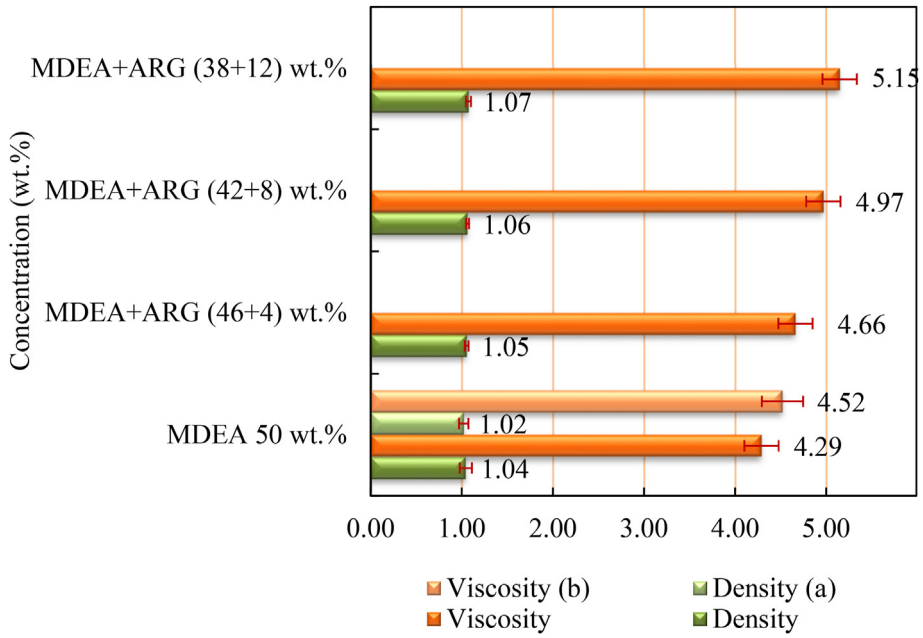

Fig. 5. The density and viscosity parameters of MDEA + ARG aqueous solutions (Literature references: [a] [40], [b] [39]).

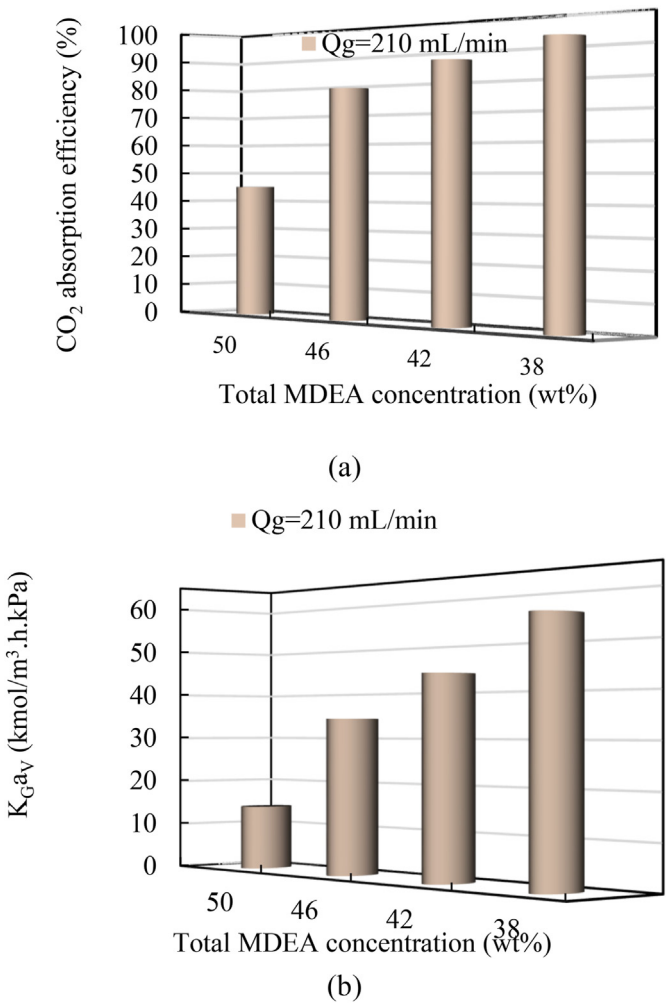

Fig. 6. The effect of MDEA and ARG concentrations on: a) CO_2 absorption efficiency, and b) Overall gas-phase mass transfer coefficient of CO_2 for Q_l = 6 mL/min.

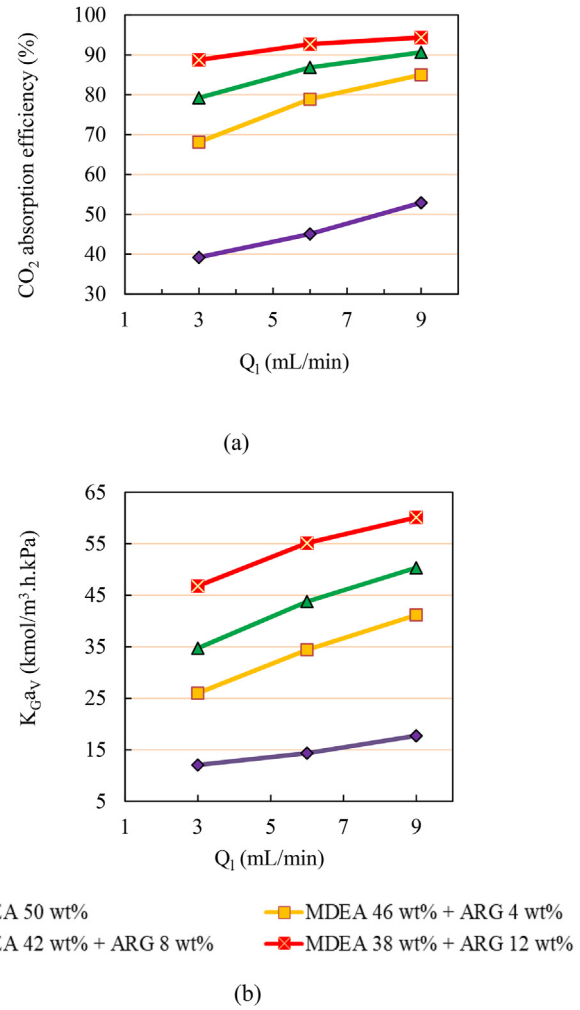

Fig. 7. a) CO_2 absorption efficiency and b) Overall gas-phase mass transfer coefficient of CO_2 versus the solvent flow rate in the microchannel at Qg = 210 mL/min.

the viscosity; based on Fig. 5, an increase in Arginine concentration from 0% to 12 wt% elevates the viscosity values within 20% and decrease the bubble velocity and the diffusion rate of CO_2, which will negatively influence the mass transfer rate in the liquid phase. Accordingly, the mass transfer performance of the CO_2 absorption into the MDEA-ARG solution counts on the competitive results of the above three influential effects.

4.4. Effect of gas flow rate (Q_g)

The impact of gaseous phase flow rate on the CO_2 absorption efficiency and $K_G a_V$ are revealed in Fig. 8. As seen, at a fixed liquid flow rate of 6 mL/min, the value of the CO_2 absorption efficiency lowers from 95.93% to 86.7% with raising the gas flow rate from 120 to 300 mL/min. For other liquid flow rates, this tendency also holds true. The reason can be described by the fact that although the specific surface area of the bubbles as well as the total effective mass transfer area gradually intensify with the gas phase flow rate, the residence time of the gas phase will be reduced in the microchannel, which raises the CO_2 concentration at the microchannel outlet. Hence, it is found that in this system, the contact time would present a greater effect on CO_2 absorption efficiency. At a higher inlet gas flow rate that the flow pattern will expand to the slug-annular flow, the rising trend of the specific surface area may level off; as such, one can expect that the MDEA and ARG molecules are hard to spread into the gas-liquid contact surface area to absorb the CO_2 molecules in the microreactor [27].

According to Fig. 8b, according to the mass transfer theory of the two-phase reaction, the values of the gas-phase mass transfer coefficient enhance as the gas flow rate increases. The most likely idea is that rising the gas flow rate provides turbulence to the gas phase, which boosts the gas velocity and the frequency of bubbles formation. This will reduce the length of the liquid slug and also the volume of the liquid phase, resulting in a reduction of the gas-side mass transfer resistance, thereby intensifying the value of the $K_G a_V$, as determined by Eq. (12) [45,46]. In this regard, the value of the $K_G a_V$ in the aqueous solution of MDEA offers a slight reduction of 14.5% with the increase of the gas flow rate from 120 to 210 mL/min, but then tends to keep constant over the period studied, when the gas flow rate exceeds 210 mL/min. This phenomenon imply that the mass transfer in the liquid phase plays a dominant role in the CO_2 absorption into the MDEA + ARG solution. Accordingly, depending on the amino acid concentration in MDEA + ARG mixture, the gas flow rate should attain a certain value i.e. the gas flow rate should be kept suitable value. Similar behaviour was showed by several researchers [46–48].

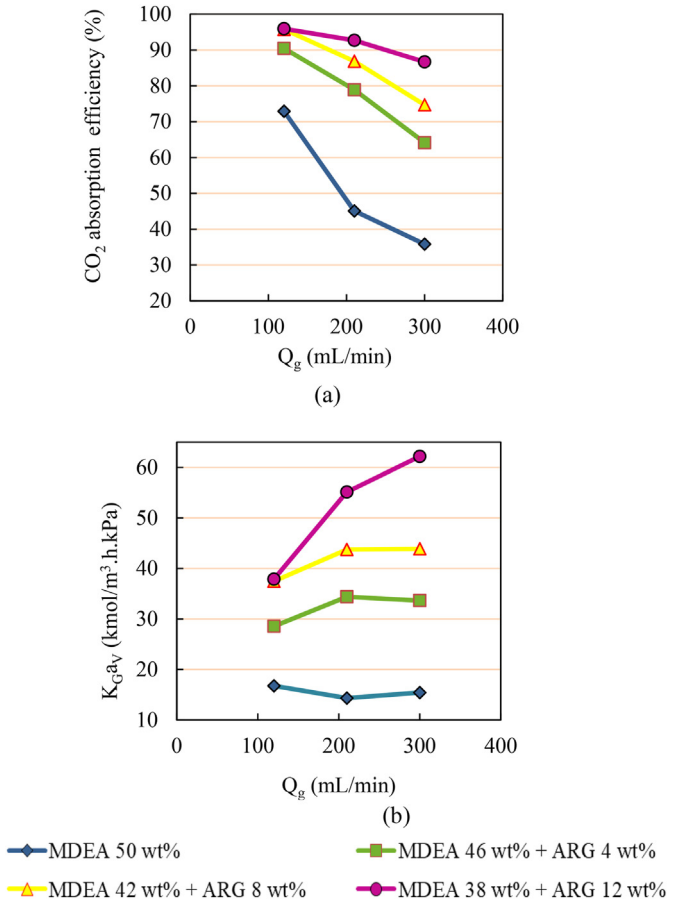

Fig. 8. Effect of gas flow rate on: a) CO_2 absorption efficiency and b) $K_G a_V$ in the microchannel with a liquid flow rate of 6 mL/min.

4.5. Volumetric mass transfer flux ($N_A a_V$)

The experimental prompter efficiency has been calculated from the ratio of the volumetric mass transfer flux with and without incorporating the $_L$-arginine. As the largest absorption efficiency (96.06%) in the current study has been occurred by the maximum concentration of the amino acid (12 wt%), the volumetric mass transfer flux ($N_A a_V$), and promoter efficiency ($N_{(M+A)}a_V/N_M a_V$) have been assessed in the binary mixture containing 12 wt% arginine. Fig. 9 represents the variations of the mass transfer flux and the prompter efficiency ($N_{(M+A)}a_V/N_M a_V$) versus the liquid and gas flow rate.

Following Fig. 9a, at a fixed Q_g of 120 mL/min, the mass transfer flux varies from 154.96 to 157.30, and 157.49 (kmol/h.m^3) for $Q_{Ll} = 3$, 6, and 9 mL/min, respectively. It is seen that the $N_A a_V$ first increase sharply and reaches and then become nearly constant. Considering this, a higher liquid flow rate provides an easier availability of the absorbent, thereby benefiting the corresponding reduction of mass-transfer resistance [49,50]. Additionally, at higher superficial liquid velocity the gas-liquid contact time will be reduced, which has an adverse effect on the CO_2 absorption. The above results exhibit that the increase in the absorbent availability has greater effects as compared to the reduction in the contact time [3]. The corresponding reduction of mass transfer resistance, caused by increasing liquid flow rate, favors the volumetric mass transfer flux of CO_2 absorption inside the microchannel.

The values of the prompter efficiency ($N_{(M+A)}a_V/N_M a_V$) reflects the strengthening effect of the presence of the amino acid. According to Fig. 9a, the rate of prompter efficiency declines from 1.43 to 1.23 with expanding the liquid flow rate from 3 to 9 mL/min. This means that although high concentrations of the amino acid will boost the driving force of the mass transfer, the positive contribution of $_L$-arginine on the volumetric mass transfer flux at low liquid flow rates is significantly higher than the high liquid flow rates.

Fig. 9b exhibits a remarkable enhancement in the trend of mass transfer flux from 157.49 to 361.82 (kmol/h.m^3), with rising the feed gas flow rate, for fixed Q_L of 9 mL/min. This behaviour can be examined relying upon the impact of the L/G ratio. As seen in the figure, a smaller liquid to gas ratio (L/G) signifies higher increase range of gas flow rate, which enhances the gas holdup and the turbulence flow regime induced by the increase of the superficial gas velocity in the system. This reflects a higher interfacial area of gas-liquid [49,51,52] and decline of contact time thereupon, hindering the chemical absorption [3], hence raising the mass transfer flux.

The results of Fig. 9b illustrates that the prompter efficiency

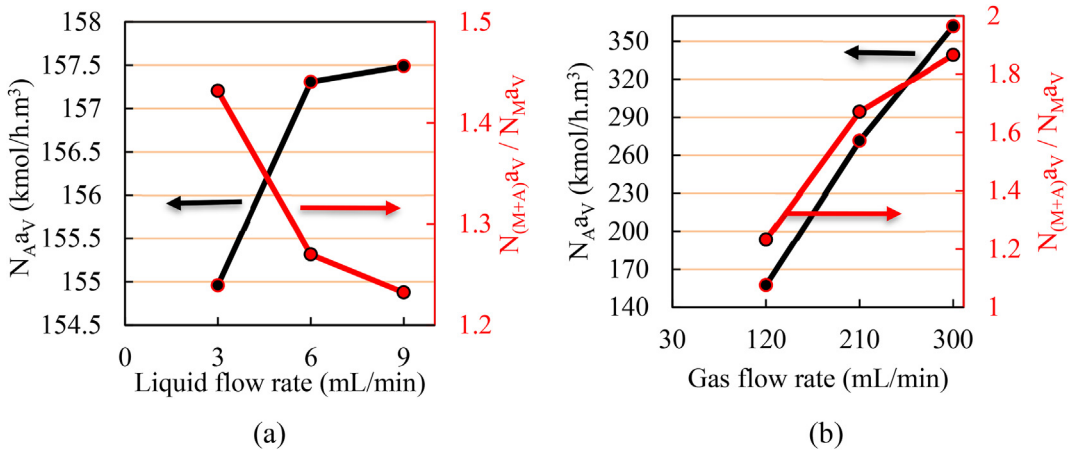

Fig. 9. Effect of (a) liquid flow rate at Q_g = 120 (mL/min), (b) gas flow rate at Q_l = 9 (mL/min) on $N_A a_V$ and promoter efficiency.

nearly rise with an increase in the gas flow rate and attains a maximum of 1.87 at Qg = 300 mL/min. Under this condition, the enhancement in the mass transfer flux with increasing the flow rate is more dominant with high concentrations of the $_L$-arginine.

4.6. Comparison with conventional systems

Table 4 reveals the values of the overall gas-phase mass transfer coefficient for previous and present studies utilizing the most common CO_2 capture mass transfer devices, including the rotating packed bed, falling film columns, packed columns and the current microreactor. From this comparison, it is apparent that in all cases that the MDEA and MEA have been utilized as the tertiary and primary alkanolamine solvents for the CO_2 capture process, the values of the $K_G a_V$ are less than that in the designed microreactor, spite the fact that there is a relatively significant difference in the

Table 4
Literature data determining $K_G a_V$, achieved by various gas-liquid absorption systems.

Contactor	solvent	Operating conditions	$K_G a_V$ (kmol/m^3.h.kPa)	Ref.
Rotating packed bed	MDEA-PZ	Solvent concentration:	0.82–4.012	[53]
Inner diameter: 7.6 cm	MEA-PZ	1 M	1.67–5.2	
Outer diameter: 16 cm	AMP-PZ	T: 305 K	0.16–5	
Height: 2 cm		Q_g: 6–10 L/min		
Rotating speed: 1300 rpm		Q_l: 50–90 cc/min		
		Gas pressure:		
		0.152 MPa		
Falling film columns	MEA	MEA concentration:	0.011–0.34	[54]
Height: 1 m		30 wt%		
Diameter: 1.39 cm		T: 298 K		
		Q_g: 1.67×10^{-5}-5×10^{-5} m^3/s		
		Q_l: 1.04×10^{-7}-4.72×10^{-7} m^3/s		
		Pressure: 1 atm		
Packed column	MDEA	Solvent concentration:	0.038–0.046	[55]
Height: 1.4 m		1–3 mol/L		
Diameter: 28 mm		T: 303–333 K		
		Q_g: 24.98–39.45 kmol/m^3.hr		
		Q_l: 3.98–9.29 m^3/m^2.h		
		Pressure:103.125 kPa		
Packed column	MDEA-MEA	MDEA/MEA concentration:	0.65–0.89	[56]
Height: 2.15 m		27/3, 25/5 and 23/7 wt%		
Diameter: 27.5×10^{-2} m		T: 294–313 K		
		Q_g: 15.99, 17.85, 18.65 kmol/m^3.hr		
		Q_l: 5 m^3/m^2.h		
		P: atmospheric		
Packed column	MDEA-[Bmim][Lys]	MDEA-AAILs concentration: 0.05–0.15	0.0941–0.1314	[57]
	MDEA-[N_{1111}][Gly]	T: 313.15 K	0.1086–0.1975	
	MDEA-[Bmim][Gly]	Q_g: 500–1500 mL/min	0.0858–0.1314	
		Q_l: 50–150 mL/min		
Packed column	MDEA-PZ	Solvent concentration: 1–3 M	0.22–4.52	[58]
Height: 1.7 m		T: 298–333 K		
Diameter: 28 mm		Q_g: 40 kmol/m^3.hr		
		Q_l: 2–8 m^3/m^2.h		
		CO_2 partial pressure: 4–16 kPa		
Microreactor	MDEA-ARG	MDEA concentration: 38–50 wt%	12.04–62.98	This work
Length: 295 mm Diameter: 800 μm		T: 45 °C		
		Q_g: 120–300 mL/min		
		Q_l: 3–9 mL/min		
		P: atmospheric pressure		

experimental conditions. As an illustration, for the packed absorption columns, the $K_G a_V$ values have been reported in the maximum order of 0.038–4.52 kmol/m^3 h kPa. Meanwhile, in the case of the present microreactor, the above-mentioned factor varies in the range of 12.04–62.98 kmol/m^3 h kPa, which is 2–4 orders of magnitude higher than that in the traditional contacting devices.

It is worth noting that the predominant role of L-arginine amino acid as a co-promoter of the conventional alkanolamines in improving the CO_2 absorption should not be overlooked, suggesting that the amino acid-based MDEA solutions elevate the overall gas-phase mass transfer performance.

5. Conclusion

The mass transfer characteristics of the CO_2 absorption has been examined into the conventional tertiary alkanolamine system, containing L-arginine, as a co-promoter in a T-junction microreactor. From the results of the physicochemical properties, it is found that the kinematic viscosity of the blended aqueous solution of MDEA-ARG increased at a constant temperature of absorption experiments (45 °C) in the following order: 0 wt% < 4 wt% < 8 wt % < 12 wt% amino-acid. Besides, the liquid viscosity raised by 1.2 times as the blend became concentrated with L-arginine. Under the constant slug-annular flow in the microchannel, the values of the absorption efficiency (*ef*) and overall volumetric mass transfer coefficient ($K_G a_V$) were stepped up as the amino acid concentration increased.

Under the current operating condition, both of e_f and $K_G a_V$ for CO_2+ MDEA + ARG system will be improved remarkably with increasing the liquid flow rate from 3 to 9 mL/min. In contrast, the rate of prompter efficiency declines from 1.43 to 1.23 with increasing Q_l. The obtained CO_2 absorption data also revealed the enhancement in $K_G a_V$, and the volumetric mass transfer flux ($N_A a_V$) values at high ranges of the gas flow rate. Besides, the enhancement in the mass transfer flux is more dominant with high concentrations of the L-arginine. The high CO_2 absorption efficiency even could be attained 96.06%, in the blended solution of (38 + 12 wt%) MDEA + ARG. The highest $K_G a_V$ was 62.98 kmol/m^3·kPa·h at 45 °C, under the aqueous MDEA + ARG (38 + 12 wt%) flow rate of 9 mL/min, and gas flow rate of 300 mL/min.

Finally, amongst various kinds of gas-liquid contacting devices utilized MDEA for the CO_2 absorption process, the present device exhibited superior performance in the presence of L-arginine amino acid as a co-promoter, suggesting that the proposed aqueous blended solution of alkanolamine-amino acid is a promising alternative for CO_2 capture processes in the microchannel.

Credit author statement

Shokouh Sarlak: Investigation, Visualization, Formal analysis, Writing - Original Draft, **Peyvand Valeh-e-Sheyda:** Conceptualization, Investigation, Methodology, Resources, Formal analysis, Writing - Review & Editing, Project administration, Supervision.

Declaration of competing interest

The authors declare the following financial interests/personal relationships which may be considered as potential competing interests: Authors would like to acknowledge the financial support of Kermanshah University of Technology for this research under Grant Number S/P/T/1189. Also, the authors gratefully acknowledge the financial support of Ilam Gas Treating Co. (IGTC), Iran [Grant Number: 9910216].

Acknowledgement

The authors would like to acknowledge the financial support of Kermanshah University of Technology (KUT) for this research under Grant Number S/P/T/1189. Also, the authors gratefully acknowledge the financial support of Ilam Gas Treating Co. (IGTC), Iran [Grant Number: 9910216].

Nomenclature

A	mole fractions of component
Arg	L-argininea
v	Interfacial area per volume, m^2/m^3
CCS	Carbon Capture and Sequestration
D	diameter
e_f	CO_2 removal efficiency
G	Gas flow rate
$K_G a_V$	overall mass transfer coefficient
L	length
L	Liquid flow rate
MDEA	Methyl diethanolamine
N	A set of data
$N_{(M+A)}a_V$	CO_2 absorption in aqueous hybrid solutions
$N_A a_V$	volumetric mass transfer flux
$N_M a_V$	CO_2 absorption in pure MDEA aqueous solutions
P	pressure of system
Q_g	Gas flow rate (mL/min)
Q_l	liquid flow rate (mL/min)
RDS	Relative standard error
T	Temperature, °C
wt%	weight percent
x	The measured data

Greek letters

μ	mean of data
σ_x	standard deviation of the entire population

References

[1] Haghtalab A, Gholami V. Carbon dioxide solubility in the aqueous mixtures of diisopropanolamine + l-arginine and diethanolamine +l-arginine at high pressures. J Mol Liq 2019;288.
[2] Rashidi H, Sahraie S. Enhancing carbon dioxide absorption performance using the hybrid solvent: diethanolamine-methanol. Energy 2021;221:119799.
[3] Pan M-Y, Qian Z, Shao L, Arowo M, Chen J-F, Wang J-X. Absorption of carbon dioxide into N-methyldiethanolamine in a high-throughput microchannel reactor. Separ Purif Technol 2014;125:52–8.
[4] Lam KF, Sorensen E, Gavriilidis A. Review on gas–liquid separations in microchannel devices. Chem Eng Res Des 2013;91(10):1941–53.
[5] Valeh-e-Sheyda P, Rashidi H, Ghaderzadeh F. Integration of commercial CO 2 capture plant with primary reformer stack of ammonia plant. J Therm Anal Calorim 2019;135(3):1899–909.
[6] Rashidi H, Mamivand S. Experimental and numerical mass transfer study of carbon dioxide absorption using Al2O3/water nanofluid in wetted wall column. Energy 2022;238:121670.
[7] Rashidi H, Valeh-e-Sheyda P. An insight on amine air-cooled heat exchanger tubes' corrosion in the bulk CO2 removal plant. Int J Greenh Gas Contr 2016;47:101–9.
[8] Liang ZH, Rongwong W, Liu H, Fu K, Gao H, Cao F, et al. Recent progress and new developments in post-combustion carbon-capture technology with amine based solvents. Int J Greenh Gas Contr 2015;40:26–54.
[9] Chen FF, Huang K, Zhou Y, Tian ZQ, Zhu X, Tao DJ, et al. Multi-molar absorption of CO2 by the activation of carboxylate groups in amino acid ionic liquids. Angew Chem 2016;128(25):7282–6.
[10] Firaha DS, Kirchner B. Tuning the carbon dioxide absorption in amino acid ionic liquids. ChemSusChem 2016;9(13):1591–9.
[11] Guo D, Thee H, Tan CY, Chen J, Fei W, Kentish S, et al. Amino acids as carbon capture solvents: chemical kinetics and mechanism of the glycine+ CO2 reaction. Energy Fuels 2013;27(7):3898–904.
[12] Hu G, Smith KH, Wu Y, Kentish SE, Stevens GW. Screening amino acid salts as rate promoters in potassium carbonate solvent for carbon dioxide absorption. Energy Fuels 2017;31(4):4280–6.
[13] Moss G, Smith P, Tavernier D. Glossary of class names of organic compounds

and reactivity intermediates based on structure (IUPAC Recommendations 1995). Pure Appl Chem 1995;67(8–9):1307–75.
[14] Yaron A, Naider F, Scharpe S. Proline-dependent structural and biological properties of peptides and proteins. Crit Rev Biochem Mol Biol 1993;28(1):31–81.
[15] Meng C, Da-ming F, Lue-lue H, Yi-shu G, Jian-lian H, Jian-xin Z, et al. A new approach to microwave food research: analyzing the electromagnetic response of basic amino acids. Innovat Food Sci Emerg Technol 2017;41:100–8.
[16] Ganapathy H, Steinmayer S, Shooshtari A, Dessiatoun S, Ohadi MM, Alshehhi M. Process intensification characteristics of a microreactor absorber for enhanced CO2 capture. Appl Energy 2016;162:416–27.
[17] Guo R, Zhu C, Yin Y, Fu T, Ma Y. Mass transfer characteristics of CO2 absorption into 2-amino-2-methyl-1-propanol non-aqueous solution in a microchannel. J Ind Eng Chem 2019;75:194–201.
[18] Lin G, Jiang S, Zhu C, Fu T, Ma Y. Mass-transfer characteristics of CO2 absorption into aqueous solutions of N-methyldiethanolamine + diethanolamine in a T-junction microchannel. ACS Sustainable Chem Eng 2019;7(4):4368–75.
[19] Ma D, Zhu C, Fu T, Yuan X, Ma Y. An effective hybrid solvent of MEA/DEEA for CO2 absorption and its mass transfer performance in microreactor. Separ Purif Technol 2020:242.
[20] Chemat F, You HJ, Muthukumar K, Murugesan T. Effect of l-arginine on the physical properties of choline chloride and glycerol based deep eutectic solvents. J Mol Liq 2015;212:605–11.
[21] Talkhan AG, Benamor A, Nasser M, El-Naas MH, El-Tayeb SA, El-Marsafy S. Absorption of CO2 in aqueous blend of methyldiethanolamine and arginine. Asia Pac J Chem Eng 2020;15(3):e2460.
[22] Mahmud N, Benamor A, Nasser M, El-Naas MH, Tontiwachwuthikul P. Reaction kinetics of carbon dioxide in aqueous blends of N-methyldiethanolamine and L-arginine using the stopped-flow technique. Processes 2019;7(2).
[23] Mahmud N, Benamor A, Nasser M, El-Naas MH, Tontiwachwuthikul P. Reaction kinetics of carbon dioxide in aqueous blends of N-methyldiethanolamine and L-arginine using the stopped-flow technique. Processes 2019;7(2):81.
[24] Aroonwilas A, Tontiwachwuthikul P. Mass transfer coefficients and correlation for CO2 absorption into 2-Amino-2-methyl-1-propanol (AMP) using structured packing. Ind Eng Chem Res 1998;37(2):569–75.
[25] Taylor R, Krishna R. Multicomponent mass transfer. John Wiley & Sons; 1993.
[26] Afkhamipour M, Mofarahi M. Review on the mass transfer performance of CO 2 absorption by amine-based solvents in low-and high-pressure absorption packed columns. RSC Adv 2017;7(29):17857–72.
[27] Gao H, Liu S, Gao G, Luo X, Liang Z. Hybrid behavior and mass transfer performance for absorption of CO2 into aqueous DEEA/PZ solutions in a hollow fiber membrane contactor. Separ Purif Technol 2018;201:291–300.
[28] Danckwerts P. Gas-liquid. London, UK: ReactionsMcGraw-Hill Book Company; 1970.
[29] Chung P-Y, Kawaji M. The effect of channel diameter on adiabatic two-phase flow characteristics in microchannels. Int J Multiphas Flow 2004;30(7–8):735–61.
[30] Ganapathy H, Shooshtari A, Dessiatoun S, Alshehhi M, Ohadi MM. Experimental investigation of enhanced absorption of carbon dioxide in diethanolamine in a microreactor. Conference experimental investigation of enhanced absorption of carbon dioxide in diethanolamine in a microreactor, vol. ASME 2013 11th international conference on nanochannels, microchannels, and minichannels.
[31] Ganapathy H, Shooshtari A, Dessiatoun S, Alshehhi M, Ohadi M. Fluid flow and mass transfer characteristics of enhanced CO2 capture in a minichannel reactor. Appl Energy 2014;119:43–56.
[32] Tortopidis P, Bontozoglou V. Mass transfer in gas-liquid flow in small-diameter tubes. Chem Eng Sci 1997;52(14):2231–7.
[33] Zhou T, Shi H, Ding X, Zhou Y. Thermodynamic modeling and rational design of ionic liquids for pre-combustion carbon capture. Chem Eng Sci 2021;229:116076.
[34] Ganapathy H, Al-Hajri E, Ohadi MM. Phase field modeling of Taylor flow in mini/microchannels, Part I: bubble formation mechanisms and phase field parameters. Chem Eng Sci 2013;94:138–49.
[35] Yue J, Luo L, Gonthier Y, Chen G, Yuan Q. An experimental investigation of gas–liquid two-phase flow in single microchannel contactors. Chem Eng Sci 2008;63(16):4189–202.
[36] Firuzi S, Sadeghi R. Simulation of carbon dioxide absorption process by aqueous monoethanolamine in a microchannel in annular flow pattern. Microfluid Nanofluidics 2018;22(10).
[37] Feng Z, Jing-Wen M, Zheng Z, You-Ting W, Zhi-Bing Z. Study on the absorption of carbon dioxide in high concentrated MDEA and ILs solutions. Chem Eng J 2012;181–182:222–8.
[38] Chemat F, Anjum H, Shariff AM, Kumar P, Murugesan T. Thermal and physical properties of (Choline chloride + urea +l-arginine) deep eutectic solvents. J Mol Liq 2016;218:301–8.
[39] Arachchige U, Aryal N, Eimer DA, Melaaen MC. Viscosities of pure and aqueous solutions of monoethanolamine (MEA), diethanolamine (DEA) and N-methyldiethanolamine (MDEA). Ann Trans Nordic Rheol Soc 2013;21:299–306.
[40] Karunarathne SS, Eimer DA, Øi LE. Density, viscosity, and excess properties of MDEA + H2O, DMEA + H2O, and DEEA + H2O mixtures. Appl Sci 2020;10(9).
[41] Shen S, Feng X, Zhao R, Ghosh UK, Chen A. Kinetic study of carbon dioxide absorption with aqueous potassium carbonate promoted by arginine. Chem Eng J 2013;222:478–87.
[42] Zhu C, Guo H, Chu C, Fu T, Ma Y. Gas-liquid distribution and mass transfer of CO2 absorption into sodium glycinate aqueous solution in parallel multichannel microreactor. Int J Heat Mass Tran 2020;157:119943.
[43] Sahraie S, Rashidi H, Valeh-e-Sheyda P. An optimization framework to investigate the CO2 capture performance by MEA: experimental and statistical studies using Box-Behnken design. Process Saf Environ Protect 2019;122:161–8.
[44] Xu B, Gao H, Luo X, Liao H, Liang Z. Mass transfer performance of CO 2 absorption into aqueous DEEA in packed columns. Int J Greenh Gas Contr 2016;51:11–7.
[45] Chen P-C, Yang M-W, Wei C-H, Lin SZ. Selection of blended amine for CO2 capture in a packed bed scrubber using the Taguchi method. Int J Greenh Gas Contr 2016;45:245–52.
[46] Fu K, Rongwong W, Liang Z, Na Y, Idem R, Tontiwachwuthikul P. Experimental analyses of mass transfer and heat transfer of post-combustion CO2 absorption using hybrid solvent MEA–MeOH in an absorber. Chem Eng J 2015;260:11–9.
[47] Xu Y, Jin B, Chen X, Zhao Y. Performance of CO2 absorption in a spray tower using blended ammonia and piperazine solution: experimental studies and comparisons. Int J Greenh Gas Contr 2019;82:152–61.
[48] Al-Sudani FT. Absorption of carbon dioxide into aqueous ammonia solution using blended promoters (MEA, MEA+ PZ, PZ+ ArgK, MEA+ ArgK). Eng Technol J 2020;38(9A):1359–72.
[49] Chen JF, Chen GZ, Wang JX, Shao L, Li PF. High-throughput microporous tube-in-tube microreactor as novel gas–liquid contactor: mass transfer study. AIChE J 2011;57(1):239–49.
[50] Zhang L-L, Wang J-X, Xiang Y, Zeng X-F, Chen J-F. Absorption of carbon dioxide with ionic liquid in a rotating packed bed contactor: mass transfer study. Ind Eng Chem Res 2011;50(11):6957–64.
[51] Yang L, Jensen KF. Mass transport and reactions in the tube-in-tube reactor. Org Process Res Dev 2013;17(6):927–33.
[52] Zhang L-L, Wang J-X, Sun Q, Zeng X-F, Chen J-F. Removal of nitric oxide in rotating packed bed by ferrous chelate solution. Chem Eng J 2012;181:624–9.
[53] Tan C-S, Chen J-E. Absorption of carbon dioxide with piperazine and its mixtures in a rotating packed bed. Separ Purif Technol 2006;49(2):174–80.
[54] Pant K, Srivastava V. Mass transport correlation for CO2 absorption in aqueous monoethanolamine in a continuous film contactor. Chem Eng Process: Process Intensif 2008;47(5):920–8.
[55] Wen L, Liu H, Rongwong W, Liang Z, Fu K, Idem R, et al. Comparison of overall gas-phase mass transfer coefficient for CO2Absorption between tertiary amines in a randomly packed column. Chem Eng Technol 2015;38(8):1435–43.
[56] Naami A, Sema T, Edali M, Liang Z, Idem R, Tontiwachwuthikul P. Analysis and predictive correlation of mass transfer coefficient KGav of blended MDEA-MEA for use in post-combustion CO2 capture. Int J Greenh Gas Contr 2013;19:3–12.
[57] Zhong Z, Liao Y, Fu D. Study on CO 2 capture by AAILs-MDEA aqueous solution in packed tower. EES (Ecotoxicol Environ Saf) 2020;450(1):012081.
[58] Saidi M. Rate-based modeling of CO2 absorption into piperazine-activated aqueous N-methyldiethanolamine solution: kinetic and mass transfer analysis. Int J Chem Kinet 2017;49(9):690–708.